Rare Metal Materials and Engineering
Volume.50, Issue.4, April 2021
Available online at **www.rmme.ac.cn**

Science Press

Cite this article as: Xiang Zhongnan,Li Zhanjiang,Huang Shuigen,et al.Effect of Sintering Temperature on Microstructure and Machining Performance of (Ti, W, Mo, Nb)(C, N)-(Co, Ni) Cermets[J].Rare Metal Materials and Engineering,2021,50(04):1179-1186.

Effect of Sintering Temperature on Microstructure and Machining Performance of (Ti, W, Mo, Nb)(C, N)-(Co, Ni) Cermets

Xiang Zhongnan[1], Li Zhanjiang[1,2,3], Huang Shuigen[4], Chang Fa[2,3], Dai Pinqiang[1,2,3]

[1] College of Materials Science and Engineering, Fuzhou University, Fuzhou 350116, China; [2] College of Materials Science and Engineering, Fujian University of Technology, Fuzhou 350118, China; [3] Fujian Provincial Key Laboratory of New Material Preparation and Forming Technology, Fuzhou 350118, China; [4] Department of Materials Engineering, KU Leuven, Brussels 1000, Belgium

Abstract: Dense Co- and Ni-bonded Ti($C_{0.6}N_{0.4}$) matrix cermets with secondary carbides, i.e., WC, Mo_2C, and NbC, were prepared by liquid phase sintering in vacuum for 60 min at temperatures ranging from 1410 to 1490 °C. The detailed microstructural and phase analysis was performed by scanning electron microscopy, electron probe microanalysis, and X-ray diffraction. The effect of sintering temperature on the microstructure, mechanical properties, and machining performance of cermets was investigated. The results show that sintering temperature has a significant impact on the microstructural characteristics of (Ti, W, Mo, Nb)(C, N)-(Co, Ni) cermets. The total carbon content of cermets decreases with increasing the sintering temperature and a carbon-deficient phase (M_6C) is observed in the cermet sintered at 1490 °C. The cermets sintered at temperatures of up to 1470 °C are composed of an fcc solid solution metal binder and two types of core-rim structured grains, i.e., cubic carbide solution and cubic Ti(C, N) solution phases. The best machining performance on continuous/interrupted turning is found in the cermet sintered at 1470 °C because of an optimum combination of hardness and transverse rupture strength.

Key words: cermet; sintering temperature; microstructure; hardness; machining

Recently, the demand for cutting tool materials has considerably increased because of the continuous upgradation of advanced machining equipment. Ti(C, N)-based cermet tools have attracted considerable attention because of their good hot hardness, excellent wear resistance and chemical stability, as well as low cost of raw materials[1-8]. Although Ti(C, N) cermets exhibit advantages in high speed machining and high surface finishing, these cermets are prone to tool chipping when they are faced with large processing capacity or interrupted cutting operations because of the inherited brittleness. Generally, the poor wettability between Ti(C, N) and binder phase is one of the primary reasons for the low fracture toughness of Ti(C, N) cermets[9-16]. Improved toughness and transverse rupture strength (TRS) are reported by modifying chemical compositions[17-19], starting powders[20-24], and sintering conditions[25-27]. The microstructure and performance of Ti(C, N)-based cermets are considerably influenced by adding secondary carbides (WC/Mo_2C/NbC/TaC)[2]. A small amount of NbC or TaC addition to Ti($C_{0.7}N_{0.3}$)-Ni systems can improve the interrupted cutting performance by retaining hot hardness and increasing the thermal shock resistance at higher temperatures[8-10]. During liquid phase sintering, carbides/nitrides added to Ti(C, N) cermets lead to the formation of core rim structure of Ti(C, N) grains as well as core rim structure of carbide-rich solution grains. Both the ceramic grain size and composition of core-rim grains can be influenced by the sintering temperature[11,26,27]. For a given composition, the sintering of Ti(C, N) cermets at high temperatures generally improves the fracture toughness and reduces the hardness[26,27]. At present, there is little available information on the machining performance of Ti(C, N)-based cermet tools which are obtained at different sintering temperatures. In this study, the effect of sintering

Received date: April 06, 2020
Foundation item: University-Industry Cooperation Project of Fujian Province (2019H6022)
Corresponding author: Dai Pinqiang, Ph. D., Professor, College of Materials Science and Engineering, Fujian University of Technology, Fuzhou 350118, P. R. China, Tel: 0086-591-22863456, E-mail: pqdai@126.com

temperature (i.e., 1410 °C to 1490 °C) on the evolution of microstructure, total carbon/nitrogen content, and especially the machining performance of (Ti, W, Mo, Nb)(C, N)-(Co, Ni) cermet tools was studied.

1 Experiment

1.1 Material preparation

In this study, the starting powders included commercial powders of Ti($C_{0.6}N_{0.4}$), WC, Mo_2C, NbC, Co, and Ni. Table 1 lists both chemical composition and particle size of the powders.

A powdered mixture with the compositions of Ti($C_{0.6}N_{0.4}$)-20WC-10Mo_2C-5NbC-8Co-7Ni (wt%) was prepared by the conventional powder metallurgy technique. The theoretical density was estimated to be 6.8 g/cm^3, and the mixture had a total C and N content of 8.0wt% and 5.1wt%, respectively. The as-received Ti($C_{0.6}N_{0.4}$) powder was initially milled for 72 h in ethanol using WC-Co milling balls to break the agglomerates, and then it was dried in a vacuum drying oven. The powder mixture was mixed on a multi-directional mixer in ethanol for 24 h using WC-6wt%Co milling balls. The ball-to-powder mass ratio was 4:1, and the slurry was then dried in a vacuum drying oven at 110 ℃. The dried powder was sieved, and then compacted into rectangular-shaped bars and TNMG160404 standard inserts at 147 MPa. As shown in Fig.1, the compacts were sintered in a graphite heating vacuum furnace using the sintering cycle. The samples were sintered for 1 h at 1410, 1430, 1450, 1470, and 1490 ℃ under a vacuum pressure <20 Pa.

1.2 Characterization

The bulk density of sintered cermets was measured in ethanol. The magnetic saturation (M_s) of cermets was measured using a SM-8100/LDJ-702 coercive force and magnetic saturation measurement instrument manufactured by Leco (St. Joseph, MI, USA). Phase identification in the sintered cermets was detected using an X'Pert PRO X-ray diffractometer (PANalytical, Eindhoven, Netherlands). The microstructure of the cermets was obtained by a Hitachi S-4800 scanning electron microscope (Hitachi, Tokyo, Japan). The elemental analysis of polished cross-sections were conducted by electron probe microanalysis (JXA-8530F, JEOL Ltd., Japan), equipped with a wavelength dispersive analysis system. The total carbon and nitrogen content of the powder mixture and sintered cermets were measured by LECO-C230 high-frequency infrared analyzer (St. Joseph, MI, USA) and EGMA-620W oxygen-nitrogen analyzer (HORIBA, Paris, France). The Vickers hardness (HV_{30}) and fracture resistance (K_{IC}) of the alloy were determined by a Tukon2100B hardness tester (Instron, Grove City, PA, USA) according to the ISO 28079:2009 standard (Hardmetals-Palmqvist Toughness Test). The HV_{30} was measured under an indentation load of 294 N for 15 s at room temperature. The K_{IC} was calculated from the length of the radial cracks around the Vickers indentations using the formula proposed by Shetty et al[28]. The transverse rupture strength (TRS) was measured on polished specimens with dimensions of 6.5 mm×5.25 mm×20 mm by a CMT5305 universal testing machine (MTS, Shenzhen, China) according to the ASTM B406 standard (Standard Test Method for Transverse Rupture Strength of Cemented Carbides). The reported values of HV_{30}, K_{IC}, and TRS are the mean and standard deviation of five measure values. Moreover, thermodynamic simulations were performed to estimate the phase constitution of the sintered cermets using Thermo-Calc[29] and a commercial Ni-based database TCNI8.

Table 1 Characteristics of the starting powders

Powders	Grain size (F_{SSS})/μm	Purity/wt%	C content/ wt%	N content/ wt%
Ti($C_{0.6}N_{0.4}$)	1.3	99.6	11.20	10.10
WC	1.3	99.6	6.14	-
Mo_2C	1.2	99.8	5.90	-
NbC	1.5	99.9	11.00	-
Co	1.0	99.6	-	-
Ni	1.2	99.9	-	-

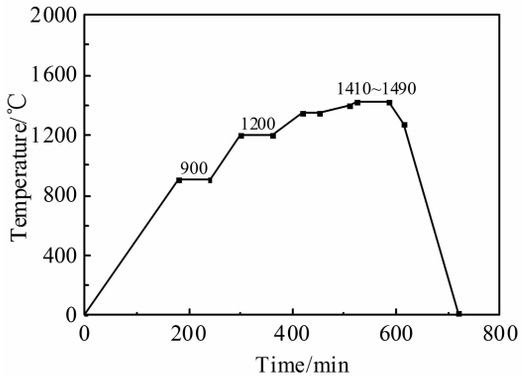

Fig.1 Representative sintering cycles of the investigated samples

The performance of cutting tool was assessed via a dry longitudinal cylindrical turning of C45 (HB140) steel, and continuous cutting was performed with a turning speed of 250 m/min, feed rate of 0.2 mm/rev, and depth of cut (ap) of 1 mm. After dry turning for 25 min, the maximum flank wear width (VBmax) was used to evaluate the wear resistance. The interrupted cutting was performed with a turning speed of 150 m/min, feed rate of 0.2 mm/rev, and depth of cut (ap) of 1.5 mm. Furthermore, the failure time of interrupted cutting was recorded, and the cutting tests were performed using three different inserts of each grade.

2 Results and Discussion

2.1 Microstructure

Fig.2a shows a representative microstructural feature of a core-rim structured Ti(C, N) cermet. Because of the addition of secondary carbides, these Co and Ni bonded Ti(C, N) cermets are primarily composed of three phases: hard phase, metal binder phase, and surrounding phase. As reported in several studies[30,31], in TiCN-based cermets, there is commonly a core-

rim structure; sometimes, the rim comprises two parts: the outer rim and the inner rim. The composition of the core in (Ti, W, Mo, Nb)(C, N)-(Co, Ni) cermets, namely, the hard phase, is believed to be TiCN, which is deemed to be the residue of un-dissolved raw materials. Furthermore, the rim, i.e., the surrounding phase, is a type of complicated (Ti, W, Mo, Nb)(C, N) solution, which has a similar crystalline structure with the core but much more heavy metal atoms than the core[3].

Fig. 2b~2f show the microstructures of the (Ti, W, Mo, Nb) (C, N) - (Co, Ni) cermets, sintered for 60 min at 1410, 1430, 1450, 1470, and 1490 ℃. In addition to the bright metallic binder, two types of core-rim structure grains, i.e., the grey contrast carbide solution grains and dark contrast Ti(C, N) rich grains, are detected in these cermets. A closer inspection of the microstructures indicates that the change in sintering temperature has a significant effect on the structural characteristics. When the sintering temperature is 1410 ℃, because of the low sintering temperature, there are still a small number of pores in the material, which indicate that the densification process is not complete. As shown by the white arrows in Fig.2b, there is aggregation of binder phase in the alloy because of the insufficient flow of the binder phase Co and Ni at a lower sintering temperature. This will result in the uneven distribution of the binder phase in the alloy. When the sintering temperature increases to 1430 ℃, the phenomenon of uneven distribution of binder phase is improved. Moreover, the binder phases are distributed in a network around the surrounding phase primarily because of the increase in sintering temperature, which promotes the fluidity of the binder phase. At this time, the pores in the materials disappear and the structure of the alloy is densified. Furthermore, after sintering at 1450 ℃, the size of hard phase reduces and becomes more uniform because of continuous dissolution, and then the surrounding phase around the hard phase is uniform and continuous. As the sintering temperature increases to 1470 ℃, the thickness of surrounding phase (rim) increases because the solubility and dissolution rate of the hard phase increase. At the sintering temperature of 1490 ℃, the thickness of surrounding phase in the material continues to increase, and the color contrast of the core phase becomes lighter because additional Ti(C, N) grains dissolve into the gray surrounding phase.

2.2 Phase analysis

Fig.3 shows the XRD patterns of (Ti, W, Mo, Nb)(C, N)-(Co, Ni) cermets sintered at different temperatures. Fig. 3 shows that Ti(C, N), (Ti, W, Mo)C and (Nb, Mo)C phases are present in the (Ti, W, Mo, Nb)(C, N)-(Co, Ni) cermets at temperatures of 1410~1490 ℃. WC, Mo_2C, and NbC components that are added in the composition completely disappear through a solid solution reaction before 1410 ℃. Thus, from Ref.[4], it can be inferred that (Ti, W, Mo, Nb)(C, N) solid solution forms with increasing the sintering temperature. Both NbC and Mo_2C tend to form a (Nb, Mo)C solid solution, while the binder phase is primarily in the form of $TiCo_3$ without a significant diffraction peak. Moreover, Fig.3 shows that Mo_2C is easy to form solid solution with other carbides in the component before the liquid phase appears, which improves the wettability between carbides and the binder phase[3].

Note that the sintering and densification of Ti(C, N) - based cermets involve complex thermodynamic and kinetic phenomena. Moreover, multiple factors, such as alloy composition and sintering cycle, have a significant influence on the microstructure, phase constitution, and properties of cermets.

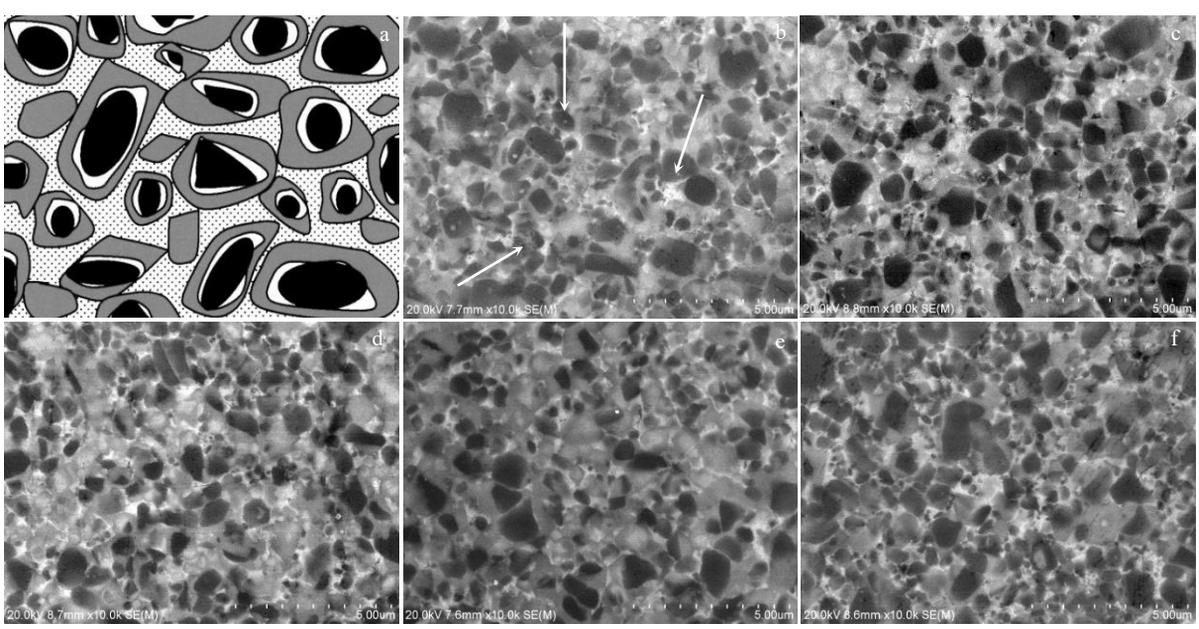

Fig.2 Microstructures of and Ti(C, N)-based cermet (a) and (Ti, W, Mo, Nb)(C, N)-(Co, Ni) cermets sintered at different temperatures for 60 min: (b) 1410 ℃, (c) 1430 ℃, (d) 1450 ℃, (e) 1470 ℃, and (f) 1490 ℃

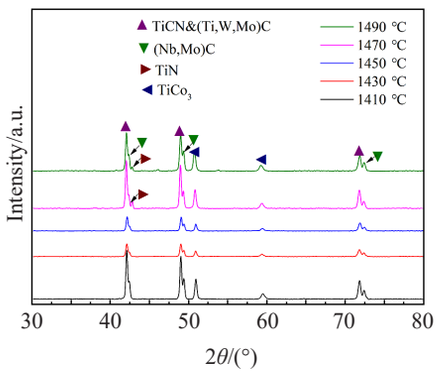

Fig.3 XRD patterns of (Ti, W, Mo, Nb)(C, N)-(Co, Ni) cermets sintered at different temperatures

In this study, a thermodynamic simulation was performed to assess the influence of the sintering temperature on the phase constitution of (Ti, W, Mo, Nb)(C, N)-(Co, Ni) cermets. Furthermore, TiC, TiN, WC, Mo_2C, NbC, Co, Ni, and C were defined as input compounds for the calculation and the vacuum pressure was set as 20 Pa. Fig.4a shows the calculated phase constitution of the (Ti, W, Mo, Nb)(C, N)-(Co, Ni) cermets sintered at different temperatures. The estimated phase constitution, i.e., the coexistence of Ti(C, N), (Ti, Nb, W, Mo)C, and binder phases, is consistent with the characterization results of phase composition in Fig.3. The sintering temperature is primarily affected by the content of carbide solution and binder phase. With increasing the sintering temperature, an additional liquid phase is formed, whereas the amount of (Ti, Nb, W, Mo)C solution phase is decreased. The experimental study by XRD (Fig.3) shows that the sintered (Ti, W, Mo, Nb)(C, N)-(Co, Ni) cermets contain a (Nb, Mo)C solid solution, which corresponds to the calculation results of Mo_2C and NbC as the primary components of carbide solution (Fig. 4c). Fig. 4d shows that the sintering temperature influences the composition of the liquid phase. With increasing the sintering temperature, more and more WC and Mo_2C dissolve in the liquid phase, whereas almost no NbC dissolves in the liquid phase. This behavior is related to the characteristics of NbC. Cubic NbC has a high surface energy, and the higher the surface energy of the material, the lower the solubility in liquid metal[32,33]. Furthermore, NbC has a very high melting point (3520 °C) and can resist high temperature softening and adhesion wear. Studies have reported that the yield strength of NbC at 1000 °C is considerably higher than that of WC[34].

2.3 Composition and properties

Table 2 shows the composition and properties of (Ti, W, Mo, Nb) (C, N)-(Co, Ni) cermets sintered at different temperatures. According to Table 2, the total carbon of the alloy slightly decreases with increasing the sintering temperature. When the sintering temperature reaches 1490 ℃, the total carbon of the alloy significantly decreases, while the variation of magnetic saturation strength (M_s) is consistent with that of total

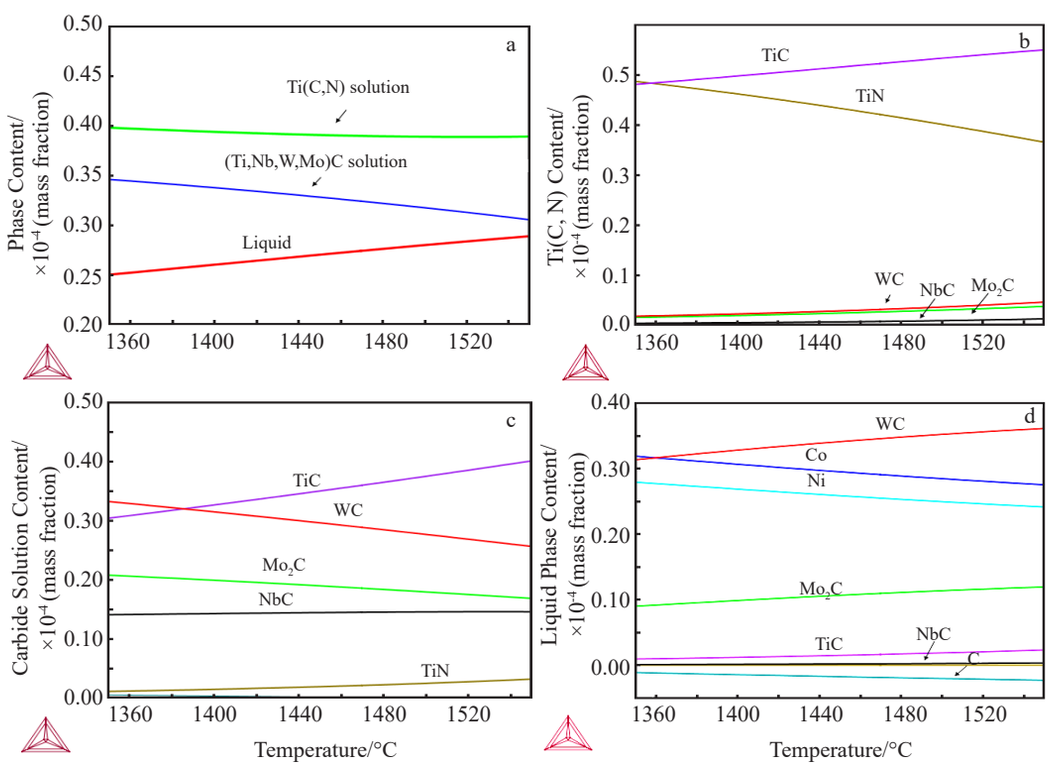

Fig.4 Influence of temperature on phase constitution of investigated cermets: (a) phase compositions, (b) composition of Ti(C,N), (c) composition of carbide solution, and (d) composition of liquid phase

Table 2 Compositions and properties of (Ti, W, Mo, Nb)(C, N)-(Co, Ni) cermets sintered at different temperatures

Sintering temperature/℃	C content/ wt%	N content/ wt%	ρ/g·cm^{-3}	Porosity	M_s/kA·m^{-1}	HV_{30}/ ×10 MPa	K_{IC}/ MPa·m$^{1/2}$	TRS/MPa
1410	7.77	4.72	6.79	A02B00C00	2.0±0.2	1689±30	7.8±0.3	2356±45
1430	7.71	4.72	6.79	A02B00C00	1.8±0.2	1620±28	7.9±0.2	2405±43
1450	7.72	4.73	6.79	A02B00C00	2.0±0.2	1610±22	7.9±0.1	2683±38
1470	7.71	4.87	6.80	A02B00C00	1.6±0.2	1609±19	8.0±0.1	2830±35
1490	7.49	4.88	6.81	A02B00C00	0.2±0.1	1530±31	7.5±0.3	2053±52

Note: total C and N content of powder mixture is 8.0wt% and 5.1wt%, respectively.

carbon of the alloy. Note that the nitrogen content of the alloy gradually increases with increasing the sintering temperature. This behavior may be attributed to the aggravation of the effect of nitrogen atmosphere on the alloy with increasing the sintering temperature.

In terms of the effect of sintering temperature on mechanical properties, with increasing the sintering temperature, HV_{30} of the alloy decreases, while K_{IC} and TRS of the alloy gradually increase. Note that HV_{30}, K_{IC}, and TRS of the alloy significantly decrease when the sintering temperature reaches 1490 °C. The variation of K_{IC} and TRS of (Ti, W, Mo, Nb)(C, N)-(Co, Ni) cermets sintered at different temperatures, as shown in Table 2, can be understood as follows. With the increase in sintering temperature, the solid solution reaction between carbides and the dissolution and precipitation reaction of carbides in the binder phase are fully carried out. This behavior is beneficial to forming the surrounding phase and strengthening the bonding strength between the hard phase and binder phase[35,36], thus improving the K_{IC} and TRS of the alloy. With further increase in sintering temperature, when the thickness of surrounding phase exceeds a certain critical value, both K_{IC} and TRS of the alloy significantly decrease because of the brittleness of the surrounding phase[37]. Furthermore, according to the characterization results of carbon content (Table 2), the carbon content of the alloy significantly decreases when sintered at 1490 °C. Moreover, it can be inferred that there is decarburized phase (η phase) in the alloy. Therefore, (Ti, W, Mo, Nb)(C,N)-(Co,Ni) cermets have an optimal mechanical properties at a specific sintering temperature, and the comprehensive mechanical properties of the cermet are the best when sintered at 1470 °C.

To further confirm the variation of mechanical properties of (Ti, W, Mo, Nb)(C, N)-(Co, Ni) cermet sintered at 1490 ℃, electron probe microanalysis was performed by a wavelength dispersive analysis system to analyze the micro-area composition of the alloy sintered at 1470 and 1490 ℃.

Fig. 5 shows the backscattered electron imaging of morphology of (Ti, W, Mo, Nb)(C, N)-(Co, Ni) cermets sintered at 1470 and 1490 ℃. Fig. 5a shows that the black hard phase is uniform and round, the grey surrounding phase is developed, and the grey-white binder phase is uniformly distributed in a network around the surrounding phase. In addition to the typical structure of cermets, a large number of white-bright phases

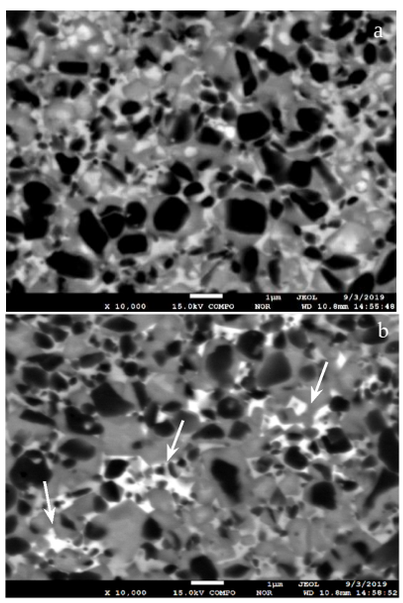

Fig.5 Backscattered electron imaging of morphology of (Ti, W, Mo, Nb)(C, N)-(Co, Ni) cermets sintered at1470 ℃ (a) and 1490 ℃ (b)

are dispersed in the matrix phase of the alloy sintered at 1490 ℃, as shown by the white arrows in Fig.5b.

The results of micro area composition analysis through wavelength dispersive spectrometer (WDS) of the alloy (Table 3) show that the total content of Ti, W, Mo and Nb in the binder phase of alloy sintered at 1470 ℃ is 40.5wt%, whereas that of alloy sintered at 1490 ℃ is 68.1wt%. Ref. [38] shows that the aggregated areas of heavy metals in cermet will be presented in the form of white-bright contrast in a back scatter electron diffraction mode, which is consistent with the characterization results in Table 3. Generally, the white-bright contrast structure under the backscatter electron diffraction mode is the decarburized phase (η phase) because of the aggregation of heavy metal elements, resulting in insufficient carbon content in cermet system. Indeed, the formation of decarburized phase (η phase) leads to the deterioration of the mechanical properties of alloys sintered at 1490 ℃, and HV_{30}, K_{IC}, and TRS of the alloy significantly decrease.

Table 3 WDS analysis of (Ti, W, Mo, Nb)(C, N)-(Co, Ni) cermets (wt%)

Element	1470 ℃			Element	1490 ℃		
	Core	Rim	Binder		Core	Rim	Binder
Ti	69.0	43.3	14.1	Ti	67.2	40.8	15.9
W	3.8	19.3	13.3	W	4.2	19.6	25.7
Mo	2.1	10.5	10.3	Mo	1.9	10.3	23.5
Nb	1.2	7.7	2.8	Nb	2.2	11.5	3.0
C	8.6	9.6	3.0	C	8.7	8.9	3.5
N	15.3	9.6	11.8	N	15.8	8.9	10.4
Co	0	0	22.7	Co	0	0	11.8
Ni	0	0	22.0	Ni	0	0	6.2
Total	100	100	100	Total	100	100	100

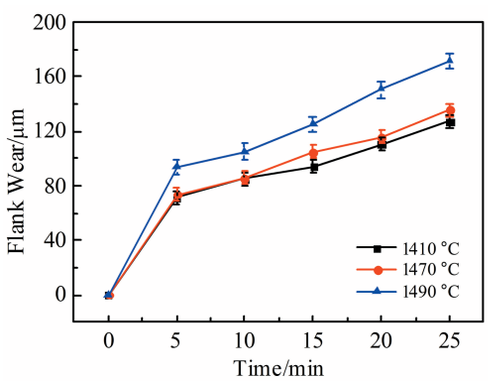

Fig.6 Flank wear of TNMG160404 inserts sintered at different temperatures during continuous cutting

2.4 Machining behavior

The (Ti, W, Mo, Nb) (C, N) - (Co, Ni) inserts (TNMG160404 type) sintered at 1410, 1470, and 1490 °C were selected for comparing the cutting performance. The experimental machine is Quick Turn Nexus 300-II MAZAK NC turning machine. Fig. 6 shows the flank wear of the TNMG160404 type inserts sintered at different temperatures during continuous cutting. Moreover, Fig. 6 shows that after continuous cutting for 25 min, the flank wear of the inserts sintered at 1410 ℃ is the smallest, followed by that of the inserts sintered at 1470 ℃ and that of the inserts sintered at 1490 ℃, which is the largest. Fig. 7 shows the morphologies of the worn flank edges of the TNMG160404 type inserts sintered at different temperatures. From Fig. 7a and 7b, it can be seen that the flank wear of inserts is considerably small, and the edge of inserts is even and smooth. However, the flank wear of the inserts in Fig. 7c is heavily worn, and the flaw is visible at the edge of the inserts. According to the properties of the alloys sintered at different temperatures in Table 2, the wear resistance of cermet inserts under continuous cutting conditions is directly related to their hardness.

Under the interrupted cutting tests, the shock resistance of inserts is considered to fail if the cutting edge cracks occur within 5 min. Table 4 shows the results of interrupted cutting tests of TNMG160404 type inserts sintered at different temperatures. From Table 4, the shock resistance of TNMG160404 type inserts sintered at 1470 ℃ is the best. According to the actual performance of cermet inserts sintered at different temperatures under continuous and interrupted cutting conditions, the comprehensive cutting performance of cermet inserts sintered at 1470 ℃ is the best in practical application conditions. This result is consistent with the optimal characterization results of the comprehensive mechanical properties of cermets sintered at 1470 ℃, which are listed in Table 2.

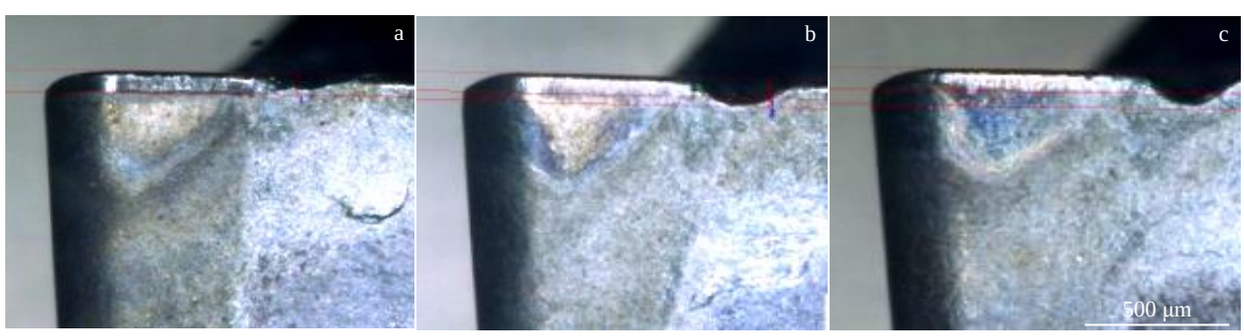

Fig.7 Morphologies of worn flank edges of the TNMG160404 inserts sintered at different temperatures during continuous cutting: (a) 1410 ℃, (b) 1470 ℃, and (c) 1490 ℃

Table 4 Results of interrupted cutting of TNMG160404 cermet inserts sintered at different temperatures

Sintering temperature/℃	Cutting time	Result
1410	3′25″	Fail
1470	5′	Qualified
1490	1′28″	Fail

3 Conclusions

1) Note that sintering temperature has a significant effect on the structure of (Ti, W, Mo, Nb)(C, N)-(Co, Ni) cermets.

With increasing the sintering temperature, the color contrast of hard phase (core) becomes lighter, the thickness of surrounding phase (rim) increases, and the solid solubility of Co(Ni) binder phase increases.

2) The total carbon of the (Ti, W, Mo, Nb)(C, N)-(Co, Ni) cermets decreases with increasing the sintering temperature. When the sintering temperature reaches 1490 ℃, the total carbon of the cermets significantly decreases, resulting in a decarburization phase (η phase) in the structure and reduces the Vickers hardness (HV_{30}), fracture resistance (K_{IC}), and transverse rupture strength (TRS) of the cermets.

3) The comprehensive cutting performance of (Ti, W, Mo, Nb)(C, N)-(Co, Ni) cermet inserts sintered at 1470 ℃ is the best for practical conditions. This result is consistent with the optimal characterization results of the comprehensive mechanical properties of cermet sintered at 1470 ℃.

References

1 Yoshimura H, Sugizawa T, Nishigaki K *et al*. *International Journal of Refractory Metals and Hard Materials*[J], 1983, 2(4): 170

2 Zackrisson J, Andrén H O, Rolander U. *Metallurgical and Materials Transactions A*[J], 2001, 32(1): 85

3 Peng Y, Miao H, Peng Z. *International Journal of Refractory Metals and Hard Materials*[J], 2013, 39: 78

4 Park Choongkwon, Nam Sangwoo, Shinhoo Kang. *Journal of Alloys and Compounds*[J], 2016, 657: 671

5 Park Choongkwon, Nam Sangwoo, Shinhoo Kang. *Materials Science and Engineering A*[J], 2016, 649: 400

6 Lin N, He Y H, Kang X Y. *Materials*[J], 2017, 10(9): 1090

7 Lengauer W, Scagnetto F. *Solid State Phenomena[*J], 2018, 274: 53

8 Huang S G, Nie H B, Guo X Y *et al*. *International Journal of Refractory Metals and Hard Materials*[J], 2019, 84: 1

9 Suzuki H, Matsubara H, Saitoh T. *Journal of the Japan Society of Powder and Powder Metallurgy*[J], 1984, 31(7): 236

10 Suzuki H, Matsubara H. *Journal of the Japan Society of Powder and Powder Metallurgy*[J], 1986, 33(4): 199

11 Matsubara H, Shin S, Sakuma T. *Solid State Phenom*[J], 1992, 25-26: 551

12 Jung J, Kang S. *Acta Materialia*[J], 2004, 52(6): 1379

13 Kwon W T, Park J S, Kim S W *et al*. *International Journal of Machine Tools and Manufacture*[J], 2004, 44(4): 341

14 Park S, Kang S. *Scripta Materialia*[J], 2005, 52(2): 129

15 Dong G B, Xiong J, Chen J Z *et al*. *International Journal of Refractory Metals and Hard Materials*[J], 2012, 35: 159

16 Yi C H, Fan H Y, Xiong J *et al*. *Ceramics International*[J], 2013, 39(1): 503

17 Ettmayer P, Kolaska H, Lengauer W *et al*. *International Journal of Refractory Metals and Hard Materials*[J], 1995, 13 (6): 343

18 Qi F, Kang S. *Materials Science and Engineering A*[J], 1998, 251(1-2): 276

19 Ahn S, Kang S. I*nternational Journal of Refractory Metals and Hard Materials*[J], 2001, 19(4-6): 539

20 Xu Zhimou, Yi Xinjian, Hu Maozhong *et al*. *Transactions of Materials and Heat Treatment*[J], 2003, 24(3): 41 (in Chinese)

21 Zhang Xiaobo, Liu Ning, Yu Chao *et al*. *Heat Treatment of Metals*[J], 2008(3): 47 (in Chinese)

22 Lv Xuepeng, Zheng Yong, Wu Peng. *Transactions of Nonferrous Metals Society of China*[J], 2011(1): 145

23 Ding Yanhong, Liu Jianwen. *Powder Metallurgy Technology* [J], 2007(4): 256 (in Chinese)

24 Zhang H A, Yi J Y, Gu S Y. *International Journal of Refractory Metals and Hard Materials*[J], 2011, 29(2): 158

25 Zackrisson J, Andrén H O. *International Journal of Refractory Metals and Hard Materials*[J],1999, 17(4): 265

26 Yan Y L, Zheng Y, Yu H J *et al*. *Powder Metallurgy and Metal Ceramics*[J], 2007, 46(9-10): 449

27 Zhou H J, Huang C Z, Zou B *et al*. *International Journal of Refractory Metals and Hard Materials*[J], 2014, 47: 71

28 Shetty D K, Wright I G, Mincer P N *et al*. *Journal of Materials Science*[J], 1985, 20(5): 1873

29 Sundman B, Jansson B, Andersson J O. *Calphad*[J], 1985, 9 (2): 153

30 Xiao S Q, Wu S H. *Cemented Carbide*[J], 2014(2): 112 (in Chinese)

31 Bao X Y, Zeng M Q, Lu Z C *et al*. *Transactions of Materials and Heat Treatment*[J], 2017, 38(5): 61 (in Chinese)

32 Krawitz A D, Crapenhoft M L, Reichel D G *et al*. *Materials Science and Engineering A*[J], 1988, 105-106: 275

33 Huang S G, Jozef V, Eduardo C *et al*. *Cemented Carbide*[J], 2018, 35(2): 69 (in Chinese)

34 Kelly A, Rowcliffe D J. *Journal of the American Ceramic Society*[J], 1967, 50(5): 253

35 Ahn S Y, Kim S W, Kang S. *Journal of the America Ceramic Society*[J], 2001, 84(4): 843

36 Park S, Kang S. *Scripta Materialia*[J], 2005, 52(2): 129

37 Xiong Weihao, Hu Zhenhua, Cui Kun. *Acta Metallurgica Sinica* [J], 1996, 32(10): 1075 (in Chinese)

38 Ahn S Y, Kang S. *Journal of the American Ceramic Society*[J], 2000, 83(6): 1489

烧结温度对(Ti, W, Mo, Nb)(C, N)-(Co, Ni)金属陶瓷组织结构和性能的影响

项忠楠[1]，李战江[1,2,3]，黄水根[4]，常　发[2,3]，戴品强[1,2,3]

(1. 福州大学 材料科学与工程学院，福建 福州 350116)

(2. 福建工程学院 材料科学与工程学院，福建 福州 350118)

(3. 福建省新材料制备与成形技术重点实验室，福建 福州 350118)

(4. 鲁汶大学 材料工程系，比利时 布鲁塞尔 1000)

摘　要：以(Ti，W，Mo，Nb)(C，N)-(Co，Ni)基金属陶瓷材料为研究对象，研究烧结温度对金属陶瓷的成分、微观组织和力学性能的影响，初步探讨成分、微观组织与材料强度的关系。结果表明：烧结温度对(Ti，W，Mo，Nb)(C，N)-(Co，Ni)基金属陶瓷组织特征有显著的影响；合金的总碳含量随着烧结温度的提高而降低，当烧结温度达到1490 ℃时，合金总碳的急剧降低，导致合金组织中出现脱碳相（η相），从而使得合金的硬度（HV_{30}）、断裂韧性（K_{IC}）和抗弯强度（TRS）降低；1470 ℃烧结温度下，(Ti，W，Mo，Nb)(C，N)-(Co，Ni)基金属陶瓷合金的HV_{30}、K_{IC}和TRS的匹配最佳，在实际应用工况下的综合切削性能最优。

关键词：金属陶瓷；烧结温度；显微组织；硬度；机加工

作者简介：项忠楠，男，1982年生，博士，高级工程师，福州大学材料科学与工程学院，福建 福州 350116，电话：0591-22863456，E-mail：1801124@163.com